Pythagorean–hodograph curves

Rida T. Farouki

Department of Mechanical and Aeronautical Engineering,
University of California, Davis, CA 95616, USA

1. PREAMBLE

With the advent of a new millenium, it seems appropriate to begin with a brief historical perspective on a topic that entails a remarkable confluence of ideas, spanning nearly 4000 years of geometry and algebra. Figure 1 shows cuneiform tablet No. 322 in the Plimpton Collection of the Rare Book & Manuscript Library, Columbia University. This compilation of sexagecimal numbers, composed in the Old Babylonian Period ($\sim$ 1900 to 1600 BC), was discovered in the 1920s and subsequently deciphered by Neugebauer and Sachs [52] in 1945. Far from being a mere financial or commercial record, the tablet reveals profound knowledge [8] of the fundamental characterization

$$a \,=\, u^2 - v^2\,, \quad b \,=\, 2uv\,, \quad c \,=\, u^2 + v^2 \tag{1}$$

for integer solutions to the "Pythagorean" equation, $a^2 + b^2 = c^2$. After a thousand years, Mesopotamian supremacy in algebra was superceded by the ascent of Greek geometry — Pythagoras of Samos ($\sim$ 560–480 BC) is credited with the first proof that this equation governs the sides of all right triangles, and is thus fundamental in distance measurement. Unfortunately, geometry fell into a prolonged stagnation after the Greeks, until Descartes' *La géométrie* of 1637 proposed a propitious marriage of geometry and algebra through the use of coordinates. Although this opened the fascinating realm of higher–order curves to mathematical scrutiny, the first steps were hesitant: Descartes blundered by categorically rejecting the idea of "rectification" (i.e., arc–length measurement) of curves.

The calculus of Leibniz and Newton resolved the existential, but not the computational, aspects of arc length measurement. Applying the Pythagorean theorem to an infinitesimal curve segment allows us to express the length of a (sufficiently smooth) parametric curve $\mathbf{r}(t) = (x(t), y(t))$ as the integral

$$s(t) \,=\, \int_0^t \sqrt{x'^2(u) + y'^2(u)}\; \mathrm{d}u\,, \tag{2}$$

but this does not, in general, admit closed–form evaluation for "simple" (rational) curves. Ideally the curve parameter *is* the arc length, $s(t) \equiv t$, an assumption that helps elucidate the intrinsic geometry of curves. It is a matter of some subtlety, however, that this ideal is unattainable by any rational curve other than a straight line [29].

Although we must relinquish the hope of rational arc–length parameterization, we can nevertheless ensure exact mensurability of the arc–length function (2) by incorporating a

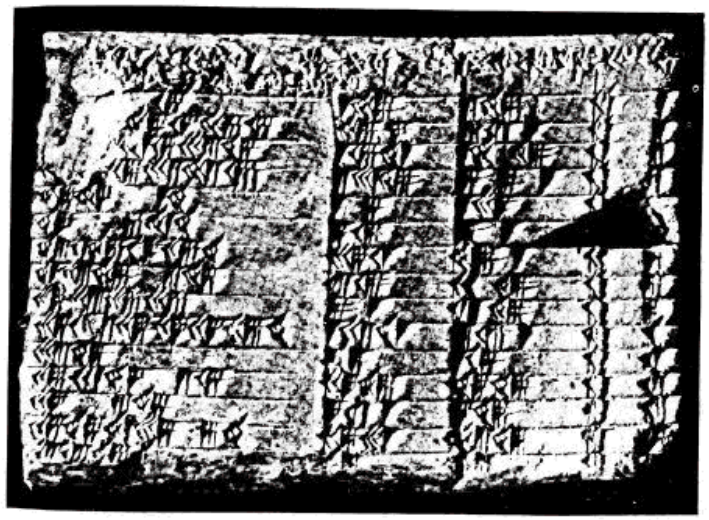

Figure 1. Plimpton 322, the cuneiform "Pythagorean triples" tablet from ancient Babylon.

special algebraic structure in the curves $\mathbf{r}(t) = (x(t), y(t))$ under consideration, based on the recognition that Pythagorean triples of *polynomials* admit the same characterization (1) as triples of *integers* [44]. Thus, by constructing curves whose hodograph (derivative) components $x'(t)$ and $y'(t)$ are elements of Pythagorean triples, we ensure reduction of the integral (2) to a polynomial in t. This is the key concept motivating the introduction [28] of Pythagorean–hodograph (PH) curves, which offer many additional advantages (rational offsets, superior shape properties, real–time interpolators, etc.), described below.

Apart from these practical advantages, the investigation of PH curves is of considerable intellectual appeal for the wealth of mathematical ideas it entails, including the geometry of complex numbers, inaugurated by Wessel, Argand, and Gauss; Hamilton's quaternions and the geometrical algebras of Clifford; medial axis transforms and the Minkowski metric of special relativity; projective geometry and dual representations; the cyclographic map and Laguerre geometry; and connections with classical geometrical optics.

2. POLYNOMIAL PH CURVES

The distinguishing feature of a polynomial PH curve $\mathbf{r}(t)$ is that the components of its hodograph $\mathbf{r}'(t)$ satisfy a Pythagorean condition, i.e., the sum of their squares is equal to the square of a polynomial $\sigma(t)$. The satisfaction of this condition entails rather different approaches in the context of planar and spatial curves, as described below.

2.1. Planar PH curves

The hodograph $\mathbf{r}'(t) = (x'(t), y'(t))$ of a planar PH curve must satisfy

$$x'^2(t) + y'^2(t) \;=\; \sigma^2(t)\,, \tag{3}$$

where $\sigma(t)$ is a polynomial. Satisfying this condition is equivalent [28] to the requirement that, in terms of polynomials $u(t)$, $v(t)$, $h(t)$, the hodograph has the form

$$x'(t) \;=\; [\,u^2(t) - v^2(t)\,]\,h(t)\,, \quad y'(t) \;=\; 2\,u(t)v(t)h(t)\,, \tag{4}$$

and hence $\sigma(t) = [\, u^2(t) + v^2(t)\,]\, h(t)$. Taking $h(t) = 1$ and $\gcd(u, v) = 1$ gives a *primitive* Pythagorean hodograph, defining a regular PH curve (i.e., $\gcd(x', y') = 1$) of odd degree.

A direct consequence of (3) is that, for a PH curve, the cumulative arc–length function (2) is just a *polynomial* (rather than an irreducible integral). Moreover, the offset curves at each distance d from $\mathbf{r}(t)$ — defined [21] by

$$\mathbf{r}_d(t) \;=\; \mathbf{r}(t) \;+\; d\,\mathbf{n}(t)\,, \tag{5}$$

where $\mathbf{n}(t)$ is the unit normal to $\mathbf{r}(t)$ — admit exact *rational* representations, eliminating the need for approximation schemes that can be inaccurate, data intensive, or lacking in robustness — see [10,57] and references therein. The exact arc length and offset properties of PH curves are extremely useful in the context of CNC machining (see §4 below).

Taking constants for $u(t)$, $v(t)$, $h(t)$ reveals the trivial fact that straight lines are PH curves. The first non–trivial examples are thus cubics, defined by choosing $h(t) = 1$ and linear polynomials $u(t)$, $v(t)$ in (4). PH cubics can be characterized geometrically in terms of their Bézier control points $\mathbf{p}_0, \ldots, \mathbf{p}_3$. Namely, if $L_k = |\mathbf{p}_k - \mathbf{p}_{k-1}|$ are the lengths of the control–polygon legs, and θ_1, θ_2 are the angles at the interior points $\mathbf{p}_1$, $\mathbf{p}_2$, the conditions

$$L_2 \;=\; \sqrt{L_3 L_1} \qquad \text{and} \qquad \theta_1 \;=\; \theta_2 \tag{6}$$

are sufficient and necessary for a PH cubic [28]. On closer scrutiny, the elegant simplicity of this characterization reveals a deeper truth: modulo rigid motions, scalings, and linear reparameterizations, PH cubics are all segments of a unique curve, *Tschirnhausen's cubic.* Since it cannot inflect, this curve is of limited value in design applications [23].

For shape flexibility similar to that of "ordinary" cubics, we must appeal to PH quintics, defined by choosing $h(t) = 1$ and quadratic polynomials $u(t)$, $v(t)$ in (4). The PH quintics can inflect and can interpolate arbitrary first–order Hermite data; they can also be used to construct C^2 splines interpolating a sequence of points (see §3). However, their control polygons do not admit simple geometrical characterizations [12], analogous to (6).

To ensure numerical stability [25,26] we always specifypolynomials in Bernstein–Bézier form on $[\,0, 1\,]$. Choosing $h(t) = 1$ and degree–m polynomials $u(t)$ and $v(t)$ with Bernstein coefficients $u_0, \ldots, u_m$ and $v_0, \ldots, v_m$ in (4) defines a PH curve $\mathbf{r}(t)$ of degree $n = 2m+1$, whose parametric speed $\sigma(t) = |\mathbf{r}'(t)|$ is a polynomial of degree $n - 1$, specified [11] by the Bernstein coefficients

$$\sigma_k \;=\; \sum_{j=\max(0,k-m)}^{\min(m,k)} \frac{\binom{m}{j}\binom{m}{k-j}}{\binom{n-1}{k}} \left(u_j u_{k-j} + v_j v_{k-j}\right), \quad k = 0, \ldots, n-1\,.$$

Integrating $\sigma(t)$, we obtain the arc–length function as a polynomial $s(t)$ of degree n with Bernstein coefficients

$$s_0 = 0 \qquad \text{and} \qquad s_k \;=\; \frac{1}{n}\sum_{j=0}^{k-1} \sigma_j\,, \quad k = 1, \ldots, n\,.$$

Note that $s(t)$ is monotone–increasing, since it is the integral of a non–negative polynomial $\sigma(t)$. Thus, although $s(t)$ does not possess a closed–form inverse [15], the parameter value t_* corresponding to any given arc length s_* can be computed to machine precision, as the

unique real root of the equation $s(t_*) = s_*$, by means of a few Newton–Raphson iterations. This property is especially useful in the formulation of real–time CNC interpolators; see §4 below. The total arc length S for $t \in [\,0,1\,]$ is simply $s_n = (\sigma_0 + \cdots + \sigma_{n-1})/n$.

To represent the offsets (5) as rational curves, we introduce homogeneous coordinates (W, X, Y) and write the control points of the PH curve $\mathbf{r}(t)$ as $\mathbf{P}_k = (1, x_k, y_k)$ for $k = 0, \ldots, n$. With $\Delta\mathbf{P}_k = \mathbf{P}_{k+1} - \mathbf{P}_k = (0, \Delta x_k, \Delta y_k)$ and

$$\Delta\mathbf{P}_k \times \mathbf{z} \;=\; (0, \Delta y_k, -\Delta x_k)\,,$$

where $\Delta x_k = x_{k+1} - x_k$, $\Delta y_k = y_{k+1} - y_k$, and $\mathbf{z}$ is a unit vector orthogonal to the plane, the offset $\mathbf{r}_d(t)$ is described by polynomials $W(t), X(t), Y(t)$ of degree $2n-1$, with Bernstein coefficients $\mathbf{O}_k = (W_k, X_k, Y_k)$ given [11] by

$$\mathbf{O}_k \;=\; \sum_{j=\max(0,k-n)}^{\min(n-1,k)} \frac{\binom{n-1}{j}\binom{n}{k-j}}{\binom{2n-1}{k}} \left(\sigma_j \mathbf{P}_{k-j} + d\, n\, \Delta\mathbf{P}_j \times \mathbf{z}\right), \quad k = 0, \ldots, 2n-1\,.$$

As the offset distance d is increased, the control points of $\mathbf{r}_d(t)$ move uniformly along fixed lines, but their "weights" W_k remain constant; see Figure 2. Although the offsets to PH curves are of higher degree, this is not problematic if we adhere to the numerically stable Bernstein form in their construction (note also that we may regard the offset as the sum of a polynomial curve of degree n and a rational curve of degree $n-1$). In §5 we shall see that the *rational* PH curves entail no increase of degree in their offsets.

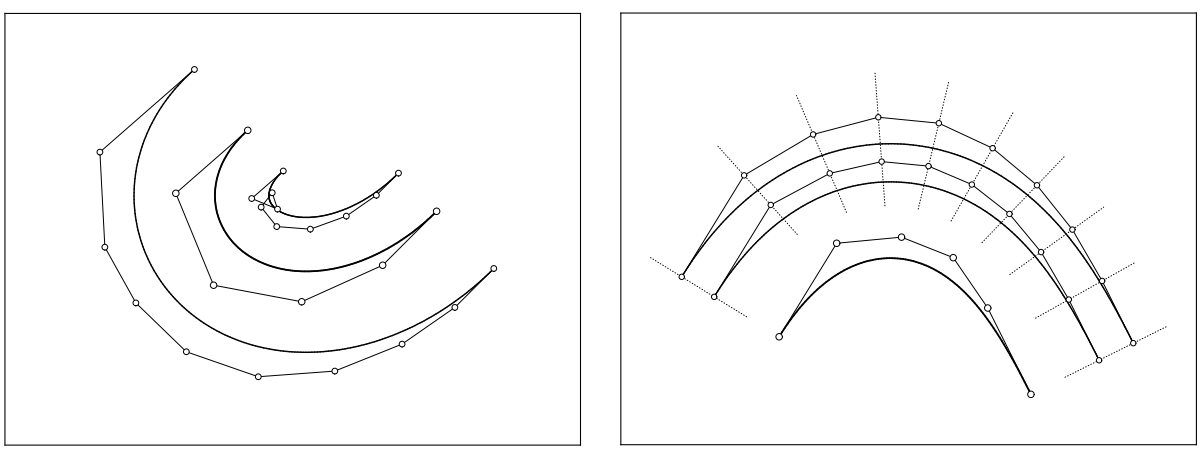

Figure 2. Left: interior and exterior offsets to a PH quintic represented exactly as rational Bézier curves of degree 9. Right: as the offset distance d is increased, the control points for successive offsets move uniformly along straight lines, and their weights remain constant.

2.2. Complex representation

By identifying points (x, y) in the plane with complex numbers $x + \mathrm{i}\, y$, any plane curve $\mathbf{r}(t) = (x(t), y(t))$ can be regarded [75] as a complex–valued function $x(t) + \mathrm{i}\, y(t)$ of a real

parameter t. For planar PH curves, this perspective proves to be extremely useful [12] — since, if $\mathbf{w}(t) = u(t) + \mathrm{i}\, v(t)$ is any complex polynomial with $\gcd(u, v) = 1$, its image

$$\mathbf{w}^2(t) \;=\; u^2(t) - v^2(t) \;+\; \mathrm{i}\, 2u(t)v(t)$$

under the conformal map $\mathbf{z} \to \mathbf{z}^2$ is a polynomial whose real and imaginary parts are elements of a primitive Pythagorean triple of the form (4), with $h(t) = 1$. Hence, in the complex representation, the (regular) PH curves are those curves whose hodographs are simply the *squares of complex polynomials*: $\mathbf{r}'(t) = \mathbf{w}^2(t)$.

The complex form plays a key role in simplifying the construction and shape analysis of planar PH curves [3,12,13,17,18,22]. Suppose, for example, that

$$\mathbf{r}(t) \;=\; \sum_{k=0}^{5} \mathbf{p}_k \binom{5}{k} (1-t)^{5-k} t^k$$

is a PH quintic in Bézier form, obtained by integrating the hodograph (4) with $h(t) = 1$ and quadratics with Bernstein coefficients u_0, u_1, u_2 and v_0, v_1, v_2 for $u(t)$ and $v(t)$. In real arithmetic, we obtain the rather cumbersome expressions

$$\begin{aligned}
(x_1, y_1) \;&=\; (x_0, y_0) \;+\; \frac{1}{5}(u_0^2 - v_0^2, 2u_0v_0)\,,\\
(x_2, y_2) \;&=\; (x_1, y_1) \;+\; \frac{1}{5}(u_0u_1 - v_0v_1, u_0v_1 + u_1v_0)\,,\\
(x_3, y_3) \;&=\; (x_2, y_2) \;+\; \frac{2}{15}(u_1^2 - v_1^2, 2u_1v_1) \;+\; \frac{1}{15}(u_0u_2 - v_0v_2, u_0v_2 + u_2v_0)\,,\\
(x_4, y_4) \;&=\; (x_3, y_3) \;+\; \frac{1}{5}(u_1u_2 - v_1v_2, u_1v_2 + u_2v_1)\,,\\
(x_5, y_5) \;&=\; (x_4, y_4) \;+\; \frac{1}{5}(u_2^2 - v_2^2, 2u_2v_2)\,,
\end{aligned}$$

for the control points[1] $\mathbf{p}_k = (x_k, y_k)$. Writing $\mathbf{p}_k = x_k + \mathrm{i}\, y_k$ and $\mathbf{w}_i = u_i + \mathrm{i}\, v_i$, on the other hand, yields the compact characterization

$$\begin{aligned}
\mathbf{p}_1 \;&=\; \mathbf{p}_0 + \frac{1}{5}\,\mathbf{w}_0^2\,,\\
\mathbf{p}_2 \;&=\; \mathbf{p}_1 + \frac{1}{5}\,\mathbf{w}_0\mathbf{w}_1\,,\\
\mathbf{p}_3 \;&=\; \mathbf{p}_2 + \frac{2\mathbf{w}_1^2 + \mathbf{w}_0\mathbf{w}_2}{15}\,,\\
\mathbf{p}_4 \;&=\; \mathbf{p}_3 + \frac{1}{5}\,\mathbf{w}_1\mathbf{w}_2\,,\\
\mathbf{p}_5 \;&=\; \mathbf{p}_4 + \frac{1}{5}\,\mathbf{w}_2^2\,.
\end{aligned} \tag{7}$$

By means of the complex form, one can easily see [12] that the set of (regular) PH curves and the set of "ordinary" (regular) polynomial curves are of the same cardinality. Familiar algorithms for the construction or modification of polynomial curves always admit analogs in terms of PH curves — although the latter are inherently non–linear, use of the complex form can greatly simplify their formulation and implementation.

[1] Note here that $\mathbf{p}_0$ is an arbitrary integration constant.

2.3. PH space curves

By analogy with (3), a PH space curve $\mathbf{r}(t) = (x(t), y(t), z(t))$ satisfies

$$x'^2(t) + y'^2(t) + z'^2(t) \;=\; \sigma^2(t)\,, \tag{8}$$

for some polynomial $\sigma(t)$. Such curves were introduced in [30], using the form

$$\begin{aligned} x'(t) &= [\,u^2(t) - v^2(t) - w^2(t)\,]\,h(t)\,, \\ y'(t) &= 2u(t)v(t)h(t)\,, \\ z'(t) &= 2u(t)w(t)h(t)\,, \end{aligned} \tag{9}$$

and hence $\sigma(t) = h(t)\,[\,u^2(t)+v^2(t)+w^2(t)\,]$. This is not, however, an entirely satisfactory spatial extension of the hodograph (4). Whereas the latter form is sufficient and necessary for a plane PH curve, the form (9) is *only sufficient* for a PH space curve. The failure of (9) to describe *all* PH space curves is apparent in the fact that this form is not invariant with respect to re–labelling of the axes (the invariance of (4) under such re–labelling can be seen by replacing (u, v) by $(\tilde{u}, \tilde{v})$, where we define $\sqrt{2}\,\tilde{u} = u + v$ and $\sqrt{2}\,\tilde{v} = u - v$).

Subsequently, a sufficient–and–necessary characterization of polynomial solutions to (8) was given in terms of polynomials $u(t)$, $v(t)$, $p(t)$, $q(t)$ by Dietz et al. [9]:

$$\begin{aligned} x'(t) &= u^2(t) + v^2(t) - p^2(t) - q^2(t)\,, \\ y'(t) &= 2u(t)p(t) + 2v(t)q(t)\,, \\ z'(t) &= 2u(t)q(t) - 2v(t)p(t)\,, \end{aligned} \tag{10}$$

and thus $\sigma(t) = u^2(t)+v^2(t)+p^2(t)+q^2(t)$. Moreover, this defines a regular PH space curve with $\gcd(x', y', z') = 1$ whenever $u(t)$, $v(t)$, $p(t)$, $q(t)$ have no common factor, whereas for (9) with $h(t) = 1$, the condition $\gcd(u, v, w) = 1$ does *not* guarantee a regular curve.

As with planar PH cubics, the twisted PH cubics can be characterized by geometrical constraints on their Bézier control polygons. In fact, the spatial PH cubics are all segments of (non–circular) helices [30] — i.e., their tangents maintain a constant angle with a given axis, and they exhibit a constant ratio of curvature to torsion.

The arc length $s(t)$ for PH space curves is obtained by a trivial extension of the methods given above for plane PH curves. The spatial analog of an offset curve is the *canal surface* with a given space curve as its spine (i.e., the envelope of a one–parameter family of fixed–radius spheres, centered on the spine curve). Since PH space curves admit orthonormal frames[2] $(\mathbf{t}, \mathbf{e}_1, \mathbf{e}_2)$ dependent rationally on t, where $\mathbf{t}$ is the tangent and $\mathbf{e}_1$, $\mathbf{e}_2$ span the normal plane, the canal surfaces with PH spine curves are rational [30]. Lü and Pottmann showed that the canal surfaces associated with *any* rational (not just PH) spine curves are, in fact, rational [47] — but their rational forms are more difficult to construct [55]. Jüttler [38,41] describes applications of PH space curves to the modelling of swept surfaces.

An important difference between planar and spatial PH curves is the lack of a compact intuitive model for the latter, analogous to the complex form of plane PH curves described in §2.2. Ueda [71] expressed PH space curves of the form (9) in terms of a special class of quaternions. For a comprehensive theory of the algebraic form of Pythagorean hodographs in spaces of different dimensions (and under different metrics), see Choi et al. [7].

[2]In general, $\mathbf{e}_1$ and $\mathbf{e}_2$ do not coincide with the principal normal $\mathbf{n}$ and binormal $\mathbf{z}$ — for a discussion of curves with rational Frenet frames, see Wagner and Ravani [72].

3. CONSTRUCTION ALGORITHMS

Since PH curves are defined by hodographs that depend on the squares and products of polynomials $u(t)$, $v(t)$, etc., the determination of coefficients for these polynomials so as to match given discrete geometrical data (points, tangents, etc.) typically incurs non–linear problems with a multiplicity of solutions.

3.1. PH quintic Hermite interpolants

The first–order Hermite interpolation problem is concerned with constructing a smooth curve, $\mathbf{r}(t)$ for $t \in [\,0,1\,]$, with given end points and derivatives: $\mathbf{r}(0) = \mathbf{p}_0$, $\mathbf{r}'(0) = \mathbf{d}_0$ and $\mathbf{r}(1) = \mathbf{p}_1$, $\mathbf{r}'(1) = \mathbf{d}_1$. As is well known, there is a unique solution among the "ordinary" cubics; to obtain sufficient degrees of freedom within the PH curves, we must appeal to the quintics [22]. It is convenient to use the complex representation, and assume[3] that $\mathbf{p}_0 = 0$ and $\mathbf{p}_1 = 1$ (note that bold characters denote points, vectors, and complex variables).

To define a PH quintic, we choose a hodograph that is the square of a complex quadratic polynomial $\mathbf{w}(t)$ expressed in Bernstein form,

$$\mathbf{r}'(t) \;=\; [\,\mathbf{w}_0(1-t)^2 + \mathbf{w}_1\, 2(1-t)t + \mathbf{w}_2 t^2\,]^2\,. \tag{11}$$

With the integration constant $\mathbf{r}'(0) = \mathbf{p}_0$, the coefficients $\mathbf{w}_0, \mathbf{w}_1, \mathbf{w}_2$ are determined by the Hermite interpolation conditions

$$\mathbf{r}'(0) \;=\; \mathbf{d}_0\,, \qquad \mathbf{r}'(1) \;=\; \mathbf{d}_1\,, \qquad \int_0^1 \mathbf{r}'(t)\,\mathrm{d}t \;=\; \mathbf{p}_1 - \mathbf{p}_0 \;=\; 1\,,$$

which yield the system of quadratic equations

$$\mathbf{w}_0^2 \;=\; \mathbf{d}_0\,, \qquad \mathbf{w}_2^2 \;=\; \mathbf{d}_1\,, \tag{12}$$

$$\mathbf{w}_0^2 \;+\; \mathbf{w}_0\mathbf{w}_1 \;+\; \frac{2\mathbf{w}_1^2 + \mathbf{w}_2\mathbf{w}_0}{3} \;+\; \mathbf{w}_1\mathbf{w}_2 \;+\; \mathbf{w}_2^2 \;=\; 5\,. \tag{13}$$

This system has a simple formal solution: equations (12) furnish two complex values for each of $\mathbf{w}_0$, $\mathbf{w}_2$ and substituting them into (13) allows the latter to be solved as a quadratic equation in $\mathbf{w}_1$. Although there are 8 solutions, they define only 4 distinct PH quintics: if $\mathbf{w}_0, \mathbf{w}_2, \mathbf{w}_1$ is a solution, so is $-\mathbf{w}_0, -\mathbf{w}_2, -\mathbf{w}_1$, and it yields exactly the same curve.

Empirically, one "good" interpolant is observed among the four distinct solutions — the others typically exhibit undesired loops or extreme curvature variations. The good interpolant may be identified as the one that minimizes a global measure of shape, such as the *absolute rotation index* or *elastic bending energy* (see Figure 3):

$$\mathcal{R}_{\mathrm{abs}} \;=\; \frac{1}{2\pi}\int_0^1 |\kappa(t)|\,|\mathbf{r}'(t)|\,\mathrm{d}t\,, \qquad \mathcal{E} \;=\; \int_0^1 \kappa^2(t)\,|\mathbf{r}'(t)|\,\mathrm{d}t\,. \tag{14}$$

The complex form facilitates exact evaluation of these quantities [13,22]. For this purpose, it is convenient to re–write the hodograph (11) as

$$\mathbf{r}'(t) \;=\; \mathbf{k}\,(t-\mathbf{a})^2(t-\mathbf{b})^2\,,$$

[3]This "standard form" for the Hermite data helps simplify the analysis — it is a trivial matter to map arbitrary Hermite data to and from it.

in terms of which the curvature can be expressed as

$$\kappa(t) \;=\; \frac{\mathrm{Im}(\overline{\mathbf{r}}'(t)\mathbf{r}''(t))}{|\mathbf{r}'(t)|^3} \;=\; \frac{2}{|\mathbf{k}|}\,\frac{\beta|t-\mathbf{a}|^2+\alpha|t-\mathbf{b}|^2}{|(t-\mathbf{a})(t-\mathbf{b})|^4}\,, \tag{15}$$

where $\alpha = \mathrm{Im}(\mathbf{a})$ and $\beta = \mathrm{Im}(\mathbf{b})$. The locations of $\mathbf{a}$ and $\mathbf{b}$ in the complex plane relative to the interval $[\,0,1\,]$ play a key role in determining the shape of PH quintics [22].

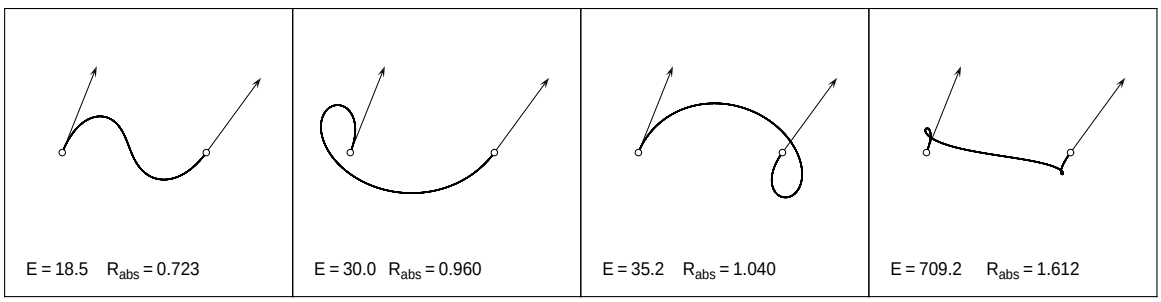

Figure 3. The four distinct PH quintic Hermite interpolants to the data $\mathbf{p}_0 = 0$, $\mathbf{p}_1 = 1$ and $\mathbf{d}_0 = 0.24 + \mathrm{i}\,0.60$, $\mathbf{d}_1 = 0.38 + \mathrm{i}\,0.52$, together with values for the bending energy and absolute rotation index (14). The derivatives have been scaled by a factor of 5 for clarity.

An alternative approach to selecting the good solution employs a qualitative criterion — "absence of anti–parallel tangents" — based on comparing the PH quintic and ordinary cubic interpolants [50]: one can show that, for "reasonable" Hermite data $\mathbf{d}_0, \mathbf{d}_1$ satisfying

$$\mathrm{Re}(\mathbf{d}_i) > 0 \qquad \text{and} \qquad |\mathbf{d}_i| < 3\,, \tag{16}$$

the "good" solution can be directly constructed by a specific choice of signs in the solution. The conditions (16) ensure that the derivatives have positive components in the direction of the displacement $\mathbf{p}_1 - \mathbf{p}_0$, and their magnitudes are commensurate with the distance $|\mathbf{p}_1 - \mathbf{p}_0| = 1$ (as would be expected in most practical applications).

3.2. Shape properties of PH quintics

A remarkable (empirical) feature of the "good" PH quintic Hermite interpolants is that they are generally of *fairer shape* — i.e., they exhibit more even curvature profiles — than the corresponding "ordinary" cubics, as is evident from the examples shown in Figure 4. This is true not only for individual Hermite segments, but also C^2 splines that interpolate a sequence of N points (see Figure 5 below). The superior curvature behavior of PH curves is advantageous not only in free–from design applications, but also in path planning for mobile robots — where physical limitations of the steering mechanism incur constraints on the allowed path curvature [5]. The curvature (15) of a PH quintic is a *rational* function of the curve parameter, with positive denominator — expressing it in Bernstein form yields an algorithm to compute rapidly–convergent bounds on the curvature of PH curves using only rational arithmetic on their coefficients [50]. Finally, note that the availability of a closed–form expression for the total arc length S and the elastic bending energy $\mathcal{E}$ in (14) opens up the possibility of quantitative "shape optimization" for PH curves [13].

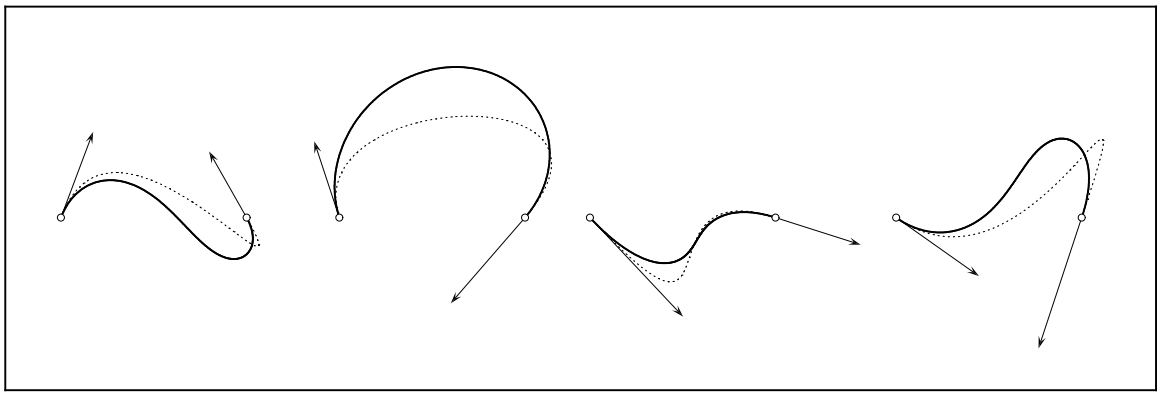

Figure 4. Comparison of "good" PH quintic (solid) and ordinary cubic (dashed) Hermite interpolants to various end derivatives $\mathbf{d}_0$ and $\mathbf{d}_1$ (shown scaled by a factor of 5 for clarity).

3.3. C^2 PH quintic splines

Apart from individual Hermite interpolants to end–point data, the ability to smoothly interpolate a sequence of points $\mathbf{p}_0, \ldots, \mathbf{p}_N$ is a common design requirement. As is well–known, C^2 cubic splines satisfy this need and incur only the solution of a tridiagonal linear system. An analogous construction is also possible [3] for C^2 PH quintic splines — the defining equations still have "bandwidth" 3, but are *complex* and *quadratic*, and thus computationally more challenging. As compensation for the greater computational cost, however, we shall see that the PH quintic splines provide much "smoother" loci (with more even curvature distributions) than their ordinary cubic counterparts.

The construction of a C^2 PH quintic spline, interpolating a sequence of $N+1$ points[4] $\mathbf{p}_0, \ldots, \mathbf{p}_N$ and satisfying specified end conditions, entails solving a system of N quadratic equations in N complex unknowns $\mathbf{z}_1, \ldots, \mathbf{z}_N$. We begin by writing the hodograph of the k–th PH quintic span $\mathbf{r}_k(t)$ of the spline curve, between $\mathbf{p}_{k-1}$ and $\mathbf{p}_k$, in the form

$$\mathbf{r}'_k(t) \;=\; \left[\tfrac{1}{2}(\mathbf{z}_{k-1}+\mathbf{z}_k)(1-t)^2 + \mathbf{z}_k\, 2(1-t)t + \tfrac{1}{2}(\mathbf{z}_k+\mathbf{z}_{k+1})t^2\right]^2, \tag{17}$$

which ensures that successive spans satisfy the continuity conditions $\mathbf{r}'_k(1) = \mathbf{r}'_{k+1}(0)$ and $\mathbf{r}''_k(1) = \mathbf{r}''_{k+1}(0)$. Assigning the integration constant $\mathbf{r}_k(0) = \mathbf{p}_{k-1}$ to this hodograph and also requiring that $\mathbf{r}_k(1) = \mathbf{p}_k$ then gives the equation

$$\begin{aligned}\mathbf{f}_k(\mathbf{z}_1, \ldots, \mathbf{z}_N) \;&=\; 3\,\mathbf{z}_{k-1}^2 \;+\; 27\,\mathbf{z}_k^2 \;+\; 3\,\mathbf{z}_{k+1}^2 \;+\; \mathbf{z}_{k-1}\mathbf{z}_{k+1} \\ &\quad+\; 13\,(\mathbf{z}_{k-1}+\mathbf{z}_{k+1})\mathbf{z}_k \;-\; 60\,\Delta\mathbf{p}_k \;=\; 0\,,\end{aligned} \tag{18}$$

where $\Delta\mathbf{p}_k = \mathbf{p}_k - \mathbf{p}_{k-1}$. Such an equation holds for each span $k = 1, \ldots, N$ of the spline curve, but the first and last equations, $\mathbf{f}_1(\mathbf{z}_1, \ldots, \mathbf{z}_N) = 0$ and $\mathbf{f}_N(\mathbf{z}_1, \ldots, \mathbf{z}_N) = 0$, must be modified to embody the prescribed end conditions. The modifications appropriate to (a) given end–derivatives $\mathbf{d}_0$, $\mathbf{d}_N$ at the points $\mathbf{p}_0$, $\mathbf{p}_N$; (b) cubic (Tschirnhausen) end spans; and (c) periodic end conditions, are described in [3].

[4]It is understood here that the points are specified in complex form, $\mathbf{p}_k = x_k + \mathrm{i}\, y_k$.

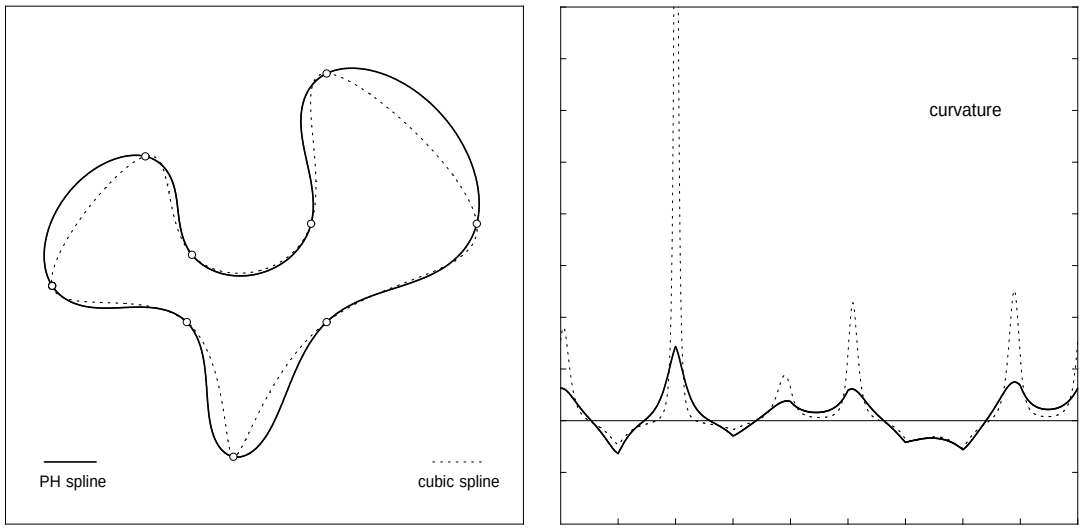

Figure 5. Comparison of C^2 PH quintic and "ordinary" C^2 cubic splines interpolating a sequence of points with uniform knots and periodic end conditions. The PH quintic spline yields a much "smoother" curve, as indicated by the curvature profiles shown on the left.

The system (18) is "tridiagonal" in the sense that each equation contains only three consecutive unknowns. Its non–linear nature, however, makes it more challenging to solve than the *linear* tridiagonal system for "ordinary" cubic splines. In general, there are 2^{N+k} distinct solutions,[5] among which one "good" PH spline may be identified (see Figure 5). For $N \leq 10$, the *homotopy method* [4,51] is a practical means to compute all solutions of this system — using a predictor–corrector method we track [3] the solutions to

$$\mathbf{h}_k(\mathbf{z}_1, \ldots, \mathbf{z}_N, \lambda) \;=\; (1-\lambda)\,\mathbf{g}_k(\mathbf{z}_1, \ldots, \mathbf{z}_N) \;+\; \lambda\,\mathbf{f}_k(\mathbf{z}_1, \ldots, \mathbf{z}_N) \;=\; 0$$

from the known solutions of a "simple" initial system, $\mathbf{g}_k(\mathbf{z}_1, \ldots, \mathbf{z}_N) = 0$ at $\lambda = 0$, to the solutions of the desired system, $\mathbf{f}_k(\mathbf{z}_1, \ldots, \mathbf{z}_N) = 0$ at $\lambda = 1$. Since the system (18) is typically well–conditioned, the homotopy method often yields convergence to machine precision. However, the cost of computing all 2^{N+k} solutions is prohibitive for $N > 10$. As an alternative, a method to compute *only* the "good" solution is described in [17], based on estimating an initial approximation to the solution (by comparison with the ordinary cubic spline), and invoking the Kantorovich conditions for guaranteed convergence [43,53,65] of the multivariate Newton–Raphson method applied to the system (18). The Kantorovich test is facilitated by the fact that, in the ∞–norm, the Jacobian matrix with elements

$$\mathbf{M}_{kl} \;=\; \frac{\partial \mathbf{f}_k}{\partial \mathbf{z}_l} \qquad \text{for } \; 1 \leq k, l \leq N$$

satisfies [17] the *global* Lipschitz condition

$$\|\, \mathbf{M}(\mathbf{x}_1, \ldots, \mathbf{x}_N) - \mathbf{M}(\mathbf{y}_1, \ldots, \mathbf{y}_N) \,\|_\infty \;\leq\; 120 \;\|\, (\mathbf{x}_1, \ldots, \mathbf{x}_N) - (\mathbf{y}_1, \ldots, \mathbf{y}_N) \,\|_\infty \,.$$

Reference [17] also presents a generalization of the system (18) to PH quintic splines with non–uniform (rather than integer) knots $t_0, \ldots, t_N$ for the points $\mathbf{p}_0, \ldots, \mathbf{p}_N$.

[5] Here $k \in \{-1, 0, +1\}$ depends on the adopted end conditions.

3.4. Geometric Hermite interpolants

Jüttler [40,41] has proposed an alternate approach to the construction of polynomial PH curves, based upon *geometric* rather than *parametric* Hermite interpolation — i.e., intrinsic geometrical properties (tangent directions, curvatures, etc.) are specified in lieu of parametric derivatives. A scheme for interpolating G^1 spatial data (points and tangent directions) by PH space cubics is described in [41], while interpolation of G^2 planar data (points, tangent directions, and curvatures) by plane PH curves of degree 7 is treated in [40]. The methods are well–suited to approximating given (non–PH) curves, from which tangents, curvatures, etc., can be computed. Conditions for (and rates of) convergence to the given curve, as the sampling interval diminishes, are also addressed.

3.5. Further constructions

Many other constructions, suited to specific applications, have been discussed by various authors. Walton and Meek consider the imposition of a curvature–monotonicity constraint on PH curves [73,74]; see also [14]. For the design of smooth cam profiles, PH curves of degree 9 have been employed as second–order Hermite interpolants [18]. Least–squares fitting of PH curves to point data has also been investigated [27], as a means of making G code part programs accessible to real–time PH curve CNC interpolators (see §4). Finally, several special PH curve contructions have been explored by Ueda [67–70].

4. REAL–TIME CNC INTERPOLATORS

Certain properties of polynomial PH curves are especially advantageous in the context of computer–numerical–control (CNC) machining. For a CNC machine to cut a specified curve[6] $\mathbf{r}(\xi)$, the tool center must follow the offset path (5) where d is the tool radius. As previously noted, PH curves (unlike general polynomial curves) have *rational* offsets, that are amenable to exact representation in CAD systems.

The ability to formulate exact *real–time interpolators*, for constant or variable feedrates, is another fundamental advantage [32] of PH curves. To produce a desired motion, a CNC machine drives several independent axes in a coordinated manner. The controller employs digital descriptions of space and time — the *sampling interval* (~ 0.001 sec) is defined by a "clock" running within the algorithm, while the *basic length unit* or spatial resolution (~ 10 microns) is determined by position encoders on each axis.

The controller compares the actual machine position (measured by the encoders) with the intended position (computed from specified paths and feedrates by the interpolator) in each sampling interval Δt — the error is used to generate control signals for the machine drives, ensuring that the desired paths and feedrates are accurately realized. The timed sequence of curve points computed by the interpolator are called *reference points*; they correspond to a discrete sampling $\xi_k = \xi(k\Delta t)$ of the solution to the differential equation

$$\sigma \frac{\mathrm{d}\xi}{\mathrm{d}t} = V\,, \tag{19}$$

where $\sigma(\xi) = |\mathbf{r}'(\xi)|$ denotes the parametric speed and $V = \mathrm{d}s/\mathrm{d}t$ is the feedrate (which may be either a constant, or dependent upon physical variables such as elapsed time t,

[6] We use ξ as the curve parameter here, since the variable t will be used to denote time.

arc length s along the path, or the local path curvature κ).

For a general polynomial curve, equation (19) does not admit a closed–form integration, even when $V =$ constant. Hence, it is common practice to use piecewise–linear/circular "G code" approximations to curved tool paths. Apart from its data–intensive nature, this approach can severely impede the ability of the machine to achieve and maintain high speeds [66]. Alternately, one may retain the analytic representation of a curved path, and use a Taylor series expansion

$$\xi_k \;=\; \xi_{k-1} \;+\; \frac{V}{\sigma}\,\Delta t \;+\; \frac{V}{\sigma^2}\left(V' - \frac{\mathbf{r}'\cdot\mathbf{r}''}{\sigma^2}\,V\right)\frac{(\Delta t)^2}{2} \;+\; \cdots \tag{20}$$

(where primes denote derivatives with respect to ξ, and σ, $\mathbf{r}'$, $\mathbf{r}''$, V, V', etc., are evaluated[7] at ξ_{k-1}) to approximate the reference points. Ordinarily, only the linear term is retained, and no attempt is made to account for the accumulation of truncation errors. Moreover, as noted in [33], this method has often been compromised in the context of variable feedrates by erroneous derivations of the appropriate Taylor coefficients.

The PH curves circumvent these problems in a simple and elegant manner: their special algebraic structure permits closed–form integration of (19) to give an equation of the form

$$F(\xi_k) \;=\; c_{k-1}\,, \tag{21}$$

where F is a monotone (usually polynomial) function, and c_k is a constant that is updated at each step. The monotonicity of F allows ξ_k to be computed to machine precision by just a few Newton–Raphson iterations, starting from ξ_{k-1}.

Complete details on PH curve interpolators can be found in [32] for feedrates that are constant or simple functions of the arc length s or curvature κ; in [19] for feedrates that maintain a constant material removal rate at fixed depth of cut along a curved path; and in [66] for any time–dependent feedrate function that has an elementary indefinite integral (the latter are especially useful in achieving smooth feed accelerations and decelerations).

Dramatic improvements in feedrate performance have been observed [66] on replacing G code interpolators by PH curve interpolators, primarily due to the "block look–ahead" problem associated with G codes. Further practical aspects concerning the use of PH curve interpolators include: conventions for specifying PH curve part programs [20]; control of cutting forces by feedrate variation [19]; path planning for contour machining of surfaces [34]; and the determination of feedrates and feed accelerations, compatible with the known torque and power capacity of the machine drives [35].

5. RATIONAL CURVES WITH RATIONAL OFFSETS

Although rational offsets are a key attribute of the polynomial PH curves, these curves are not the only "simple" curves that possess rational offsets. Lü [45,46] has shown that by suitable (improper) re–parameterizations, certain polynomial curves — whose hodographs are not Pythagorean — also admit rational offsets. Moreover, it seems natural to extend the domain of enquiry and ask: what is the complete set of *rational* curves whose offsets

[7] A varying feedrate V should be specified as a function of a physically meaningful variable (e.g., time t, arc length s, or curvature κ) rather than the curve parameter ξ. Accordingly, the quantity $V' = \mathrm{d}V/\mathrm{d}\xi$ in (20) must be cast in terms of derivatives with respect to such a variable — see [33] for complete details.

are rational? The theory of rational PH curves, as developed by Pottmann [59] and Fiorot and Gensane [36], addresses this problem conclusively. We can only skim the surface of this elegant theory — the reader should consult the references for complete details.

5.1. Rational PH curves

A basic difference is apparent upon turning our attention from polynomial PH curves to rational PH curves. Whereas the former can be constructed by integrating *any* polynomial hodograph satisfying the Pythagorean condition (3), this fact does not extend to rational PH curves: a rational hodograph satisfying (3) does not necessarily define a rational PH curve (transcendental terms may arise on integrating rational functions). Thus, a different approach to the construction of rational PH curves is advantageous.

A rational curve $\mathbf{r}(t) = (x(t), y(t))$ can be specified by homogeneous point coordinates $W(t), X(t), Y(t)$ such that $x(t) = X(t)/W(t)$, $y(t) = Y(t)/W(t)$. Alternately, we can use homogeneous line coordinates $K(t), L(t), M(t)$ such that the curve tangent at each point t is described by

$$K(t) \,+\, L(t)\,x \,+\, M(t)\,y \,=\, 0\,. \tag{22}$$

As shown by Pottmann [59], the latter approach is preferable in the theory of rational PH curves. Such curves have rational unit normals $\mathbf{n}(t) = (n_x(t), n_y(t))$ expressed in terms of polynomials $u(t)$, $v(t)$ with $\gcd(u, v) = 1$ by

$$n_x(t) \,=\, \frac{u^2(t) - v^2(t)}{u^2(t) + v^2(t)}\,, \quad n_y(t) \,=\, \frac{2u(t)v(t)}{u^2(t) + v^2(t)}\,.$$

Now the tangent line can also be written in the form

$$n_x(t)\,x \,+\, n_y(t)\,y \,=\, f(t)\,, \tag{23}$$

where $f(t)$ specifies the (signed) distance of the tangent line from the origin: this function must be rational, since $(x, y) = (x(t), y(t))$ satisfies equation (23). Now we may, without loss of generality, set $[\,u^2(t)+v^2(t)\,]\,f(t) = -\,p(t)/q(t)$, where $p(t)$ and $q(t)$ are polynomials with $\gcd(p, q) = 1$. Comparing (22) and (23), we see that rational PH curves are defined by line coordinates of the form

$$K(t) : L(t) : M(t) \,=\, p(t) \,:\, [\,u^2(t) - v^2(t)\,]\,q(t) \,:\, 2u(t)v(t)q(t)\,. \tag{24}$$

Writing $\mu = \max(\deg(u), \deg(v))$ and $\nu = \max(\deg(p), \deg(q))$, this defines a rational PH curve of class[8] $m = 2\mu + \nu$. The corresponding point coordinates can be derived [59] as

$$\begin{aligned}
W(t) \,&=\, 2\,[\,u^2(t) + v^2(t)\,]\,[\,u(t)v'(t) - u'(t)v(t)\,]\,q^2(t)\,,\\
X(t) \,&=\, 2\,[\,u'(t)v(t) + u(t)v'(t)\,]\,p(t)q(t) \,-\, 2u(t)v(t)\,[\,p'(t)q(t) - p(t)q'(t)\,]\,,\\
Y(t) \,&=\, [\,u^2(t) - v^2(t)\,]\,[\,p'(t)q(t) - p(t)q'(t)\,] \,-\, 2\,[\,u(t)u'(t) - v(t)v'(t)\,]\,p(t)q(t)\,,
\end{aligned} \tag{25}$$

from which we deduce that the rational PH curve is of order $n = 4\mu + 2\nu - 2$.

[8]The *class* (the degree of the line representation) indicates the number of curve tangents incident with any point in the plane, and the *order* (the degree of the point representation) indicates the number of curve points incident with any line in the plane [62].

Clearly, the dual line representation (24) is much simpler than the point representation (25). Algorithms for the design or construction of rational PH curves, analogous to those described in §3 for polynomial PH curves, thus rely exclusively [1,58,60,64] on the rational dual Bézier form, introduced by Hoschek [37]. The offsets to rational PH curves can be easily constructed, by noting that their tangent lines are parallel to those of the original curve at corresponding points. Writing $f(t)+d$ on the right in equation (23) amounts to simply displacing the tangent parallel to itself by distance d. Hence, by the definition of $p(t)$ and $q(t)$, the offset at distance d from a rational PH curve is obtained by replacing $p(t)$ with $p(t) - d\,[\,u^2(t)+v^2(t)\,]\,q(t)$ in (24) or (25). This has the remarkable consequence that the offsets to a rational PH curve all have the *same* degree as that curve; recall that the offsets to a (regular) degree–n polynomial PH curve are of degree $2n-1$.

The arc–length function (2) is another important difference between the polynomial and rational PH curves. For polynomial PH curves, $s(t)$ is *always* a polynomial. For rational PH curves, however $s(t)$ is not always a rational function: although the parametric speed is rational, transcendental terms may arise in its integral. Pottmann [59] has shown that any rational PH curve for which $s(t)$ is rational must be the *evolute*[9] of a rational PH curve and its family of offsets. Conversely, rational PH curves can be characterized as the *involutes* to rational curves with rational arc–length functions $s(t)$.

An elegant exposition of the theory of rational PH curves in the context of Laguerre geometry was subsequently developed by Peternell and Pottmann [56,61] — this reveals interesting connections between rational PH curves and the *caustics* and *anticaustics* of geometrical optics [16], as emphasized in the theory of rational PH curves developed [36] by Fiorot and Gensane. Unlike the polynomial PH curves, rational PH curves also admit a natural generalization to rational surfaces with rational offsets [59], although practical design schemes for such surfaces are not easy to formulate — see, however, [39,42,54]. For a detailed reconciliation of the properties of polynomial and rational PH curves, and a comparison of their relative advantages, see [24].

5.2. Improper parameterizations

For PH curves, the parameterization (5) of the offset is induced by that of the original curve $\mathbf{r}(t)$. It is conceivable, however, that polynomial curves exist whose offsets are not rational in the original curve parameter, but become rational under a re–parameterization. This circumstance was completely characterized by Lü, who showed [45,46] that, in the complex representation, it corresponds to complex polynomial hodographs of the form

$$\mathbf{r}'(t) \;=\; (\mathbf{k}\,t+1)\,\mathbf{w}^2(t)\,h(t)\,, \tag{26}$$

where $h(t)$ is a real polynomial, $\mathbf{w}(t) = u(t) + \mathrm{i}\,v(t)$ is a complex polynomial, and $\mathbf{k}$ is a complex constant. Clearly, expression (26) subsumes the polynomial PH curves as the special case $\mathbf{k}=0$. The simplest examples with $\mathbf{k}\neq 0$ are those with $\mathbf{w}(t)=1$ and $h(t)$ either a constant or linear polynomial; they define a parabola and cuspidal cubic. These curves admit rational re–parameterizations that correspond to double tracings: once in the "forward" direction, and once in "reverse." In terms of these improper parameterizations

[9]The evolute of a given curve is the locus of its centers of curvature (or, equivalently, the envelope of its normals). A locus whose evolute is a given curve is called an involute of that curve — there is an infinite family of involutes, which are all offsets of each other.

the *two–sided offset curve*, at distance $\pm d$, is found to admit a rational parameterization of degree 6 for the parabola and 8 for the cuspidal cubic; see [31,45,46].

A subset of the curves with hodographs of the form (26) are *algebraically rectifiable* [63] — i.e., the arc length is given by the square root of a polynomial in the curve parameter. Writing $f(t) = |\,\mathbf{k}\,t + 1|^2$, the condition for algebraic rectifiability of the curve defined by (26) is that

$$h(t)\,[\,u^2(t) + v^2(t)\,] \;=\; 3f'(t)g(t) \;+\; 2f(t)g'(t)$$

must hold [46,63] for some polynomial $g(t)$ — the cuspidal cubic, for example, satisfies this condition, but the parabola does not.

6. MINKOWSKI PH CURVES

Thus far, we have defined PH curves in terms of the Euclidean metric in two and three dimensions. In some application contexts, it is also advantageous to consider curves that exhibit the PH property under certain special, non–Euclidean metrics.

6.1. Minkowski metric of special relativity

The *Minkowski metric* of special relativity characterizes the distance between points in a "pseudo–Euclidean" *space–time*, spanned by one temporal and n spatial dimensions. With $n = 2$, for example, the distance d between the two points or "events" (x_1, y_1, t_1) and (x_2, y_2, t_2) is given by

$$d^2 \;=\; (x_2 - x_1)^2 + (y_2 - y_1)^2 - c^2(t_2 - t_1)^2\,, \tag{27}$$

where c is the speed of light. Events are said to have *space*–like, *time*–like, or *light*–like separation, according to whether $d^2 > 0$, $d^2 < 0$, or $d^2 = 0$. It is convenient to employ time and distance units in which $c = 1$: the Minkowski metric (27) then differs from the usual metric $d^2 = (x_2 - x_1)^2 + (y_2 - y_1)^2 + (z_2 - z_1)^2$ of Euclidean space (x, y, z) only in the *subtraction*, rather than the addition, of the last term: we say that the Euclidean and Minkowksi metric have *signatures* $(+\,+\,+)$ and $(+\,+\,-)$, respectively.

Moon [48,49] showed that Pythagorean hodographs in the Minkowski metric are very useful in recovering the boundary of a planar domain $\mathcal{D}$ from its *medial axis transform* (MAT). The medial axis is the locus of centers of maximal disks, touching the boundary $\partial\mathcal{D}$ in at least two points, that can be inscribed within the domain $\mathcal{D}$. If $\mathbf{c}(t) = (x(t), y(t))$ is a parameterization of the medial axis, we may superpose a *radius function* $r(t)$ on it, specifying the size of maximal disks centered on $\mathbf{c}(t)$: the MAT is the three–dimensional locus $(x(t), y(t), r(t))$. Introducing the unit vector

$$\mathbf{m}(t) \;=\; \frac{(\,-r'(t)x'(t) \mp \ell(t)y'(t)\,,\; -r'(t)y'(t) \pm \ell(t)x'(t)\,)}{x'^2(t) + y'^2(t)}\,,$$

where $\ell(t) = \sqrt{x'^2(t) + y'^2(t) - r'^2(t)}$ is the parametric speed of the MAT in the Minkowski metric, the envelope of the one–parameter family of circles described by $(x(t), y(t), r(t))$ has the parameterization [48]:

$$\mathbf{e}(t) \;=\; \mathbf{c}(t) \;+\; r(t)\,\mathbf{m}(t)\,.$$

Clearly, $\mathbf{e}(t)$ is not a rational locus, unless we ensure that the MAT hodograph satisfies the (Minkowski) Pythagorean condition

$$x'^2(t) + y'^2(t) - r'^2(t) = \sigma^2(t) \tag{28}$$

for some polynomial $\sigma(t)$. Moon has shown that a MAT hodograph of the form

$$\begin{aligned} x'(t) &= u^2(t) - v^2(t) - p^2(t) + q^2(t)\,, \\ y'(t) &= 2u(t)p(t) - 2v(t)q(t)\,, \\ r'(t) &= 2u(t)q(t) - 2v(t)p(t)\,, \end{aligned} \tag{29}$$

and hence $\sigma(t) = u^2(t) - v^2(t) + p^2(t) - q^2(t)$, is a sufficient and necessary condition [49] for the satisfaction of equation (28). Thus, MATs with hodographs of the form (29) are called *Minkowski Pythagorean–hodograph* (MPH) *curves.*[10]

Note that, apart from signs, the hodographs (10) and (29) for PH space curves and MPH medial axis transforms have essentially the same structure — the sign differences ensure satisfaction of the Pythagorean conditions (8) and (28) under Euclidean and Minkowski metrics; see also [7]. The reconstruction of a rational domain boundary (and of rational offsets to the boundary) from an MPH MAT is discussed in [6].

6.2. Minkowski metric defined by convex indicatrix

A generalization of the PH property to a different non–Euclidean metric, also associated with the mathematician/physicist Hermann Minkowski, was introduced by Ait Haddou et al. in [2]. They consider the geometry of the *Minkowski plane* whose metric is defined by choosing as "unit circle" a strictly–convex, centrally–symmetric locus $\mathcal{U}$. In terms of this *indicatrix*, the distance between points $\mathbf{x}$ and $\mathbf{y}$ is given by

$$d_{\mathcal{U}}(\mathbf{x},\mathbf{y}) = 2\,\frac{\|\,\mathbf{x}-\mathbf{y}\,\|}{\|\,\mathbf{x}'-\mathbf{y}'\,\|}\,, \tag{30}$$

where $\mathbf{x}'-\mathbf{y}'$ is the diameter of $\mathcal{U}$ parallel to $\mathbf{x}-\mathbf{y}$, and $\|\cdot\|$ is the usual Euclidean metric. Ait Haddou et al. give characterizations of curves whose $\mathcal{U}$–offsets, under the metric (30), are rational — they call such curves *Minkowski isoperimetric–hodograph curves.*

7. CLOSURE

By virtue of their special algebraic structure, Pythagorean–hodograph curves provide *exact* solutions to a number of basic geometrical problems in computer–aided design and manufacturing. Apart from the issues of accuracy and data volume, the primary attraction of such exact solutions lies in the enhanced *robustness* of their software embodiment.

Since its inception [28] about a decade ago, the Pythagorean hodograph concept and its various extensions and generalizations have been remarkably fertile fields for further research and practical applications. We have only been able to sketch a bare outline of all these developments, and it seems fitting to conclude by citing the "grand unified theory" of PH curves developed by Choi et al. [7], which employs the Clifford algebra perspective to gain insight into the algebraic structures — such as (4), (10), and (29) — incurred by the PH condition in various spaces of practical interest.

[10] It is universally agreed, even in Europe, that the speed σ of an MPH curve should always be specified in miles–per–hour (never kilometers–per–hour).

REFERENCES

1. R. Ait Haddou and L. Biard (1995), G^2 approximation of an offset curve by Tschirnhausen quartics, in *Mathematical Methods for Curves and Surfaces* (M. Daehlen, T. Lyche, and L. L. Schumaker, eds.), Vanderbilt Univ. Press, 1–10.
2. R. Ait Haddou, L. Biard, and M. A. Slawinsky (2000), Minkowski isoperimetric–hodograph curves, *Computer Aided Geometric Design*, to appear.
3. G. Albrecht and R. T. Farouki (1996), Construction of C^2 Pythagorean–hodograph interpolating splines by the homotopy method, *Advances in Computational Mathematics* **5**, 417–442.
4. E. L. Allgower and K. Georg (1990), *Numerical Continuation Methods: An Introduction*, Springer, Berlin.
5. H. Bruyninckx and D. Reynaerts (1997), Path planning for mobile and hyper–redundant robots using Pythagorean–hodograph curves, Proceedings, International Conference on Advanced Robotics, Monterey, CA, 595–600.
6. H. I. Choi, C. Y. Han, H. P. Moon, K. H. Roh, and N–S. Wee (1999), Medial axis transform and offset curves by Minkowski Pythagorean hodograph curves, *Computer Aided Design* **31**, 59–72.
7. H. I. Choi, D. S. Lee, and H. P. Moon (2000), Clifford algebra, spin representation, and rational parameterization of curves and surfaces, preprint.
8. D. J. de Solla Price (1964), The Babylonian "Pythagorean triangle" table, *Centaurus* **10**, 219–231.
9. R. Dietz, J. Hoschek, and B. Jüttler (1993), An algebraic approach to curves and surfaces on the sphere and other quadrics, *Computer Aided Geometric Design* **10**, 211–229.
10. G. Elber, I–K. Lee, and M–S. Kim (1997), Comparing offset curve approximation methods, *IEEE Computer Graphics and Applications* **17** (3), 62–71.
11. R. T. Farouki (1992), Pythagorean–hodograph curves in practical use, in *Geometry Processing for Design and Manufacturing* (R. E. Barnhill, ed.), SIAM, Philadelphia, 3–33.
12. R. T. Farouki (1994), The conformal map $z \to z^2$ of the hodograph plane, *Computer Aided Geometric Design* **11**, 363–390.
13. R. T. Farouki (1996), The elastic bending energy of Pythagorean–hodograph curves, *Computer Aided Geometric Design* **13**, 227–241.
14. R. T. Farouki (1997), Pythagorean–hodograph quintic transition curves of monotone curvature, *Computer Aided Design* **29**, 601–606.
15. R. T. Farouki (2000), Convergent inversion approximations for polynomials in Bernstein form, *Computer Aided Geometric Design* **17**, 179–196.
16. R. T. Farouki and J–C. A. Chastang (1992), Curves and surfaces in geometrical optics, in *Mathematical Methods in Computer Aided Geometric Design II* (T. Lyche and L. L. Schumaker, eds.), Academic Press, Boston, 239–260.
17. R. T. Farouki, B. K. Kuspa, C. Manni, and A. Sestini (2000), Efficient solution of the complex quadratic tridiagonal system for C^2 PH quintic splines, preprint.
18. R. T. Farouki, J. Manjunathaiah, and S. Jee (1998), Design of rational cam profiles with Pythagorean–hodograph curves, *Mechanism and Machine Theory* **33**, 669–682.

19. R. T. Farouki, J. Manjunathaiah, D. Nicholas, G.–F. Yuan, and S. Jee (1998), Variable feedrate CNC interpolators for constant material removal rates along Pythagorean–hodograph curves, *Computer Aided Design* **30**, 631–640.
20. R. T. Farouki, J. Manjunathaiah, and G.–F. Yuan (1999), G codes for the specification of Pythagorean–hodograph tool paths and associated feedrate functions on open–architecture CNC machines, *International Journal of Machine Tools and Manufacture* **39**, 123–142.
21. R. T. Farouki and C. A. Neff (1990), Analytic properties of plane offset curves & Algebraic properties of plane offset curves, *Computer Aided Geometric Design* **7**, 83–99 & 101–127.
22. R. T. Farouki and C. A. Neff (1995), Hermite interpolation by Pythagorean–hodograph quintics, *Mathematics of Computation* **64**, 1589–1609.
23. R. T. Farouki and J. Peters (1996), Smooth curve design with double–Tschirnhausen cubics, *Annals of Numerical Mathematics* **3**, 63–82.
24. R. T. Farouki and H. Pottmann (1996), Polynomial and rational Pythagorean–hodograph curves reconciled, in *The Mathematics of Surfaces VI* (G. Mullineux, ed.), Oxford Univ. Press, 355–378.
25. R. T. Farouki and V. T. Rajan (1987), On the numerical condition of polynomials in Bernstein form, *Computer Aided Geometric Design* **4**, 191–216.
26. R. T. Farouki and V. T. Rajan (1988), Algorithms for polynomials in Bernstein form, *Computer Aided Geometric Design* **5**, 1–26.
27. R. T. Farouki, K. Saitou, and Y–F. Tasi (1998), Least–squares tool path approximation with Pythagorean–hodograph curves for high–speed CNC machining, in *The Mathematics of Surfaces VIII* (R. Cripps, ed.), Information Geometers, Winchester, 245–264.
28. R. T. Farouki and T. Sakkalis (1990), Pythagorean hodographs, *IBM Journal of Research and Development* **34**, 736–752.
29. R. T. Farouki and T. Sakkalis (1991), Real rational curves are not "unit speed," *Computer Aided Geometric Design* **8**, 151–157.
30. R. T. Farouki and T. Sakkalis (1994), Pythagorean–hodograph space curves, *Advances in Computational Mathematics* **2**, 41–66.
31. R. T. Farouki and T. W. Sederberg (1995), Analysis of the offset to a parabola, *Computer Aided Geometric Design* **12**, 639–645.
32. R. T. Farouki and S. Shah (1996), Real–time CNC interpolators for Pythagorean–hodograph curves, *Computer Aided Geometric Design* **13**, 583–600.
33. R. T. Farouki and Y–F. Tsai (2000), Exact Taylor series coefficients for variable–feedrate CNC curve interpolators, *Computer Aided Design*, to appear.
34. R. T. Farouki, Y–F. Tsai, and G–F. Yuan (1998), Contour machining of free–form surfaces with real–time PH curve CNC interpolators, *Computer Aided Geometric Design* **16**, 61–76.
35. R. T. Farouki, Y–F. Tsai, and C. S. Wilson (2000), Physical constraints on feedrates and feed accelerations along curved tool paths, *Computer Aided Geometric Design* **17**, 337–359.
36. J. C. Fiorot and T. Gensane (1994), Characterization of the set of rational curves with rational offsets, in *Curves and Surfaces in Geometric Design* (P. J. Laurent,

A. Le Méhauté, and L. L. Schumaker, eds.), AK Peters, Wellesley, MA, 153–160.
37. J. Hoschek (1983), Dual Bézier curves and surfaces, in *Surfaces in Computer Aided Geometric Design* (R. E. Barnhill and W. Boehm, eds.), North Holland, Amsterdam, 147–156.
38. B. Jüttler (1998), Generating rational frames of space curves via Hermite interpolation with Pythagorean hodograph cubic splines, in *Geometric Modeling and Processing '98*, Bookplus Press, 83–106.
39. B. Jüttler (1998), Triangular Bézier surface patches with a linear normal vector field, in *The Mathematics of Surfaces VIII* (R. Cripps, ed.), Information Geometers, Winchester, 431–446.
40. B. Jüttler (2000), Hermite interpolation by Pythagorean hodograph curves of degree seven, *Mathematics of Computation*, to appear.
41. B. Jüttler and C. Mäurer (1999), Cubic Pythagorean hodograph spline curves and applications to sweep surface modeling, *Computer Aided Design* **31**, 73–83.
42. B. Jüttler and M. L. Sampoli (2000), Hermite interpolation by piecewise polynomial surfaces with rational offsets, *Computer Aided Geometric Design* **17**, 361–385.
43. L. V. Kantorovich and G. P. Akilov (1982), *Functional Analysis* (2nd edition), Pergamon Press, Oxford.
44. K. K. Kubota (1972), Pythagorean triples in unique factorization domains, *American Mathematical Monthly* **79**, 503–505.
45. W. Lü (1994), Rationality of the offsets to algebraic curves and surfaces, *Applied Mathematics* **9** (Ser. B), 265–278.
46. W. Lü (1995), Offset–rational parametric plane curves, *Computer Aided Geometric Design* **12**, 601–616.
47. W. Lü and H. Pottmann (1996), Pipe surfaces with rational spine curve are rational, *Computer Aided Geometric Design* **13**, 621–628.
48. H. P. Moon (1998), Computing rational offsets via medial axis transform using polynomial speed curves in $\mathbf{R}^{2,1}$, in *Geometric Modeling and Processing '98*, Bookplus Press, 187–203.
49. H. P. Moon (1999), Minkowski Pythagorean hodographs, *Computer Aided Geometric Design* **16**, 739–753.
50. H. P. Moon, R. T. Farouki, and H. I. Choi (2000), Construction and shape analysis of PH quintic Hermite interpolants, *Computer Aided Geometric Design*, to appear.
51. A. P. Morgan (1987), *Solving Polynomial Systems Using Continuation for Engineering and Scientific Problems*, Prentice–Hall, Englewood Cliffs, NJ.
52. O. Neugebauer and A. J. Sachs (1945), *Mathematical Cuneiform Texts*, American Oriental Series Vol. 29, American Oriental Society, New Haven.
53. J. M. Ortega (1968), The Newton–Kantorovich theorem, *American Mathematical Monthly* **75**, 658–660.
54. M. Peternell and H. Pottmann (1996), Designing rational surfaces with rational offsets, in *Advanced Topics in Multivariate Approximation* (F. Fontanella, K. Jetter, and P. J. Laurent, eds.), World Scientific Press, 275–286.
55. M. Peternell and H. Pottmann (1997), Computing rational parameterizations of canal surfaces, *Journal of Symbolic Computation* **23**, 255–266.
56. M. Peternell and H. Pottmann (1998), A Laguerre geometric approach to rational

offsets, *Computer Aided Geometric Design* **15**, 223–249.
57. B. Pham (1992), Offset curves and surfaces: a brief survey, *Computer Aided Design* **24**, 223–229.
58. H. Pottmann (1994), Applications of the dual Bézier representation of rational curves and surfaces, in *Curves and Surfaces in Geometric Design* (P. J. Laurent, A. Le Méhauté, and L. L. Schumaker, eds.), AK Peters, Wellesley, MA, 377–384.
59. H. Pottmann (1995), Rational curves and surfaces with rational offsets, *Computer Aided Geometric Design* **12**, 175–192.
60. H. Pottmann (1995), Curve design with rational Pythagorean–hodograph curves, *Advances in Computational Mathematics* **3**, 147–170.
61. H. Pottmann and M. Peternell (1998), Applications of Laguerre geometry in CAGD, *Computer Aided Geometric Design* **15**, 165–186.
62. E. J. F. Primrose (1955), *Plane Algebraic Curves*, Macmillan, London.
63. T. Sakkalis and R. T. Farouki (1993), Algebraically rectifiable parametric curves, *Computer Aided Geometric Design* **10**, 551–569.
64. R. Schickentanz (1997), Interpolating G^1 splines with rational offsets, *Computer Aided Geometric Design* **14**, 881–885.
65. R. A. Tapia (1971), The Kantorovich theorem for Newton's method, *American Mathematical Monthly* **78**, 389–392.
66. Y–F. Tsai, R. T. Farouki, and B. Feldman (2000), Performance analysis of CNC interpolators for time–dependent feedrates along PH curves, *Computer Aided Geometric Design*, submitted.
67. K. Ueda (1997), Deformation of plane curves preserving Pythagorean hodographs, *Proceedings of the 1997 IEEE Conference on Information Visualization*, IEEE Computer Society, 71–76.
68. K. Ueda (1998), Spherical Pythagorean–hodograph curves, in *Mathematical Methods for Curves and Surfaces II* (M. Daehlen, T. Lyche, and L. L. Schumaker, eds.), Vanderbilt Univ. Press, 485–492.
69. K. Ueda (1998), Pythagorean–hodograph curves on isothermal surfaces, in *The Mathematics of Surfaces VIII* (R. Cripps, ed.), Information Geometers, Winchester, 339–353.
70. K. Ueda (1998), Helical curves over Pythagorean–hodograph curves, in *Geometric Modeling and Processing '98*, Bookplus Press, 115–128.
71. K. Ueda (1998), Pythagorean–hodograph space curves by quaternion calculus, preprint.
72. M. G. Wagner and B. Ravani (1997), Curves with rational Frenet–Serret motion, *Computer Aided Geometric Design* **15**, 79–101.
73. D. J. Walton and D. S. Meek (1996), A Pythagorean–hodograph spiral, *Computer Aided Design* **29**, 943–950.
74. D. J. Walton and D. S. Meek (1998), G^2 curves composed of planar cubic Pythagorean hodograph quintic spirals, *Computer Aided Geometric Design* **15**, 547–566.
75. C. Zwikker (1963), *The Advanced Geometry of Plane Curves and Their Applications*, Dover, New York (reprint).